IRSTI 538.93 https://doi.org/10.26577/ijmph.2023.v14.i2.01

Suman Sharma and Shalini Jain*

University of Rajasthan, Jaipur, India-302004
E-mail: s9549170542@gmail.com, drshalinijainshah@gmail.com
(Received 26 September 2023; received in revised form 26 October 2023; accepted 28 October 2023)

Numerical analysis of electromagnetic trihybrid nanofluid flow in a convectively heated permeable channel

Abstract: This research aims to examine the tri-hybrid nanofluid flow in a convectively heated permeable channel with the effect of heat generation/absorption. Tri-hybrid nanofluid is formed by suspending three different nanoparticles namely, aluminium oxide (Al_2O_3), copper (Cu) and nickel (Ni) in the base fluid water (H_2O). For stability of the fluid transverse magnetic and electric fields are considered in the fluid model. The aim of this work is to carry out a comparative study for the heat transfer enhancement of base fluid with mono (Al_2O_3), hybrid (Al_2O_3+Cu) and ternary ($Al_2O_3+Cu+Ni$) nanofluids. This study is implicated in those fields which are dealing with extreme heat or cold conditions, aerospace technology, biosensors, nano-drugs and metal coatings. The boundary layer equations that govern the flow are transformed to dimension-free form by appropriate transformable variables and then solved by using bvp4c program in MATLAB software. It is found that the fluid flow resist by magnetic parameter and assist by electric field, while the thermal profiles rise by enhancing the value of these parameters. Furthermore, numerical outcomes for skin-friction coefficient and Nusselt number are deliberated in graphical form. Thus, it is concluded that, ternary hybrid nanofluid enhances the thermal conductivity of the base fluid more than to traditional or hybrid nanofluid.
Key words: Trihybrid nanofluid, electric field, magnetic field, convection, heat generation/absorption.

1. Introduction

Several researchers have observed that the mono-nanofluid significantly increases the potential to enhance heat transfer properties compared to traditional base fluids such as water, oils, ethylene glycol etc.[1]–[10]. Mono nanofluid is a combination of base fluid with solid nano particles such as carbon, silver, alumina oxide, copper, titanium oxide etc. Although, Mono-nanofluids have wide range of applications in industries, including electronics cooling, automotive engine cooling, solar thermal systems, and industrial processes where efficient heat transfer is crucial, but have some limitations. For example metallic nanoparticles such as *Ag, Cu, Al* have very high thermal conductivity but they are unstable due to high reactivity, while the non-metallic nanoparticles as CuO, MgO, Al_2O_3 have more stability but low conductivity. These limitations inspired the researchers to form better nanofluids, with this a new concept of hybrid or tri-hybrid nanofluid came into existence. Hybrid and tri-hybrid nanofluids refer to the combination of different types of nanoparticles within a single base fluid. It is concluded in many studies that the inclusion of Al_2O_3 nanoparticles in hybrid nanofluids, significantly enhances the thermal conductivity of base fluid [11]–[20] . Tri-hybrid nanofluids are designed to exhibit superior thermal conductivity, optimal viscosity and enhanced heat transfer performance. Xuan et al. [21] experimentally investigate the stability and non-Newtonian characteristic of tri-hybrid nanofluid Al_2O_3-TiO_2-Cu/water. Thakur and Sood [22] analyzed a computational model for Al_2O_3-Cu-Ni/water over a convectively heated Riga plate. Guedri et al. [23] investigated tri-hybrid nanofluid MgO-Cu-$MWCNT$/water past a stretching surface with the impact of Joule heating. Mahmood et al. [24] studied tri-hybrid nanofluid Al_2O_3-TiO_2-Cu/water past a non-linear permeable stretching/shrinking surface. Guedri et al. [25] examined flow of ternary hybrid nanofluid Cu-TiO_2-Al_2O_3/H_2O towards a non-linear stretching sheet. Das et al. [26] focused on electro-osmotic convective flow of Cu-Ag-Al_2O_3/H_2O ternary hybrid nanofluid in a vertical channel. Bilal et al. [27] studied the effect of Soret and Dufour on ternary hybrid nanofluid in a 3D computational domain. Ramesh et al. [28] analyzed heat source/sink effect in a convergent/divergent stretchable channel. Rauf et al. [29] presented a study for MHD micropolar ternary nanofluid Fe_3O_4-Al_2O_3-TiO_2/H_2O between two parallel sheets with hall current and morphological effects. Manjunatha et al. [30] studied convective heat transfer in TiO_2-SiO_2-

Al_2O_3/H_2O ternary nanofluid past a stretching sheet. Abideen et al. [31] analyzed the impact of activation energy in MHD tri-hybrid nanofluid flow through porous surface.

Fluid flow in permeable channel is significant due to its broad applications in engineering, biomedicine and in daily life as ground water flow, filtration, printing papers etc. Many researchers have numerically investigated nanofluid flow in a channel. Najafabadi et al. [32] investigated nanofluid flow in a vertical channel with polynomial boundary conditions. Maiti et al. [33] studied mass suction and injection effect on hybrid nanofluid flow between two parallel plates. Raza et al. and Kumari et al. [34], [35] studied Casson fluid flow in a permeable channel. Siddique et al. [36] analyzed the effect of heat source/sink in a Channel. Zheng et al. [37] investigated the influence of shape of vortex generator on a nanofluid flow in a channel. Zeeshan et al. [38] studied non-thermal conductivity on nanofluid flow in a channel. Ahmed et al. [39] analyzed Cu/H_2O nanofluid with pressure drop characteristics in a channel. Verma et al. [40] explored heat transfer enhancement in a channel using hybrid nano particles *Cu* and Al_2O_3. Tlili et al. [41] studied MHD flow of Couette-Poiseuille nanofluid in a permeable channel.

In recent years, researchers considered electro-magnetic fluid flow due to their significant applications in MHD power generation, aerospace, biomedical, space propulsion system etc. Asogwa et al. [42] investigated Casson nanofluid over an electromagnetic plate. Wakif et al. [43] investigated suction and Joule heating effects on EMHD fluid flow over a moving Riga plate. Bhatti et al. [44] analyzed electromagnetohydrodynamic flow of third grade fluid. Tian et al. [45]studied electrokinetic effects on EMHD flows. Rashid et al. [46] examined the impact of Knudsen number on EMHD flow. Algehyne et al. [47] studied effects of chemical reaction and velocity slip on EMHD nanofluid flow along a Riga plate. Khatun et al. [48] studied suction effect on EMHD fluid flow over a Riga plate.

From a comprehensive literature review, it has been revealed that no investigation has been conducted on the flow of ternary hybrid nanofluid of Al_2O_3, *Cu* and *Ni* in a channel till date. The composition of ternary hybrid nanofluid is made by submerging Al_2O_3, *Cu* and *Ni* in the base fluid H_2O. This composition was stable because of non-reactivity of the nanoparticle Al_2O_3 with nanoparticles of *Cu* and *Ni*. For more stability of the fluid the electric and transverse magnetic fields are considered in the fluid model. The aim of this work is to carry out a comparative study for the heat transfer enhancement of traditional nanofluid with hybrid and ternary nanofluid. The results for various pertinent physical parameters are examined through graphs and tables for velocity and temperature.

2. Mathematical Formulation

We have considered the flow of two dimensional, steady incompressible ternary hybrid nanofluid with the effect of heat generation/absorption in a permeable channel. Coordinate system is taken in such way that the x-axis is along the centreline of the channel and y-axis is parallel to it. Lower and upper plate of the channel is located at $y=-h/2$ and $y=h/2$ respectively. The composition of ternary hybrid nanofluid is made by submerging Al_2O_3, *Cu* and *Ni* in the base fluid H_2O. A transverse magnetic field B_0 and electrical field E_0 stabilize the fluid is acting in y-direction. The temperature is maintained constant and symbolized by T_0 and T_h at lower and upper plate respectively.

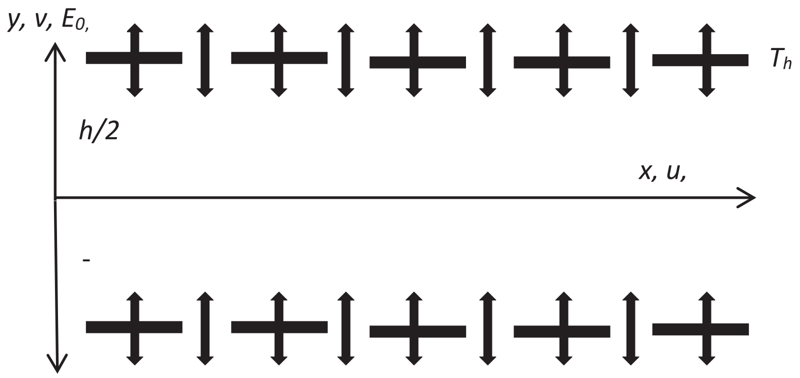

Figure 1 – Coordinate system and schematic diagram of the flow problem

The relevant governing equations to the problem are given by:

Continuity equation

$$\frac{\partial u}{\partial x}+\frac{\partial v}{\partial y}=0 \tag{1}$$

Momentum equation

$$u\frac{\partial u}{\partial x}+v\frac{\partial u}{\partial y}=-\frac{1}{\rho_{thnf}}\frac{\partial p}{\partial x}+\upsilon_{thnf}\frac{\partial^2 u}{\partial y^2}-$$
$$-\frac{\sigma_{thnf}}{\rho_{thnf}}B_0^2u-\frac{\sigma_{thnf}}{\rho_{thnf}}E_0B_0\pm g\beta_{thnf}(T-T_h) \tag{2}$$

$$u\frac{\partial v}{\partial x}+v\frac{\partial v}{\partial y}=-\frac{1}{\rho_{thnf}}\frac{\partial p}{\partial y}+\upsilon_{thnf}\frac{\partial^2 v}{\partial x^2} \tag{3}$$

Energy equation

$$u\frac{\partial T}{\partial x}+v\frac{\partial T}{\partial y}=-\frac{k_{thnf}}{(\rho c_p)_{thnf}}\frac{\partial^2 T}{\partial y^2}+$$
$$+\frac{Q_0}{(\rho c_p)_{thnf}}(T-T_h)+$$
$$+\frac{\sigma_{thnf}}{(\rho c_p)_{thnf}}(uB_0-E_0)^2 \tag{4}$$

With the boundary conditions

$$At\ y=0, \frac{\partial u}{\partial y}=0, v=0, T=T_0$$
$$At\ y=\frac{h}{2}, u=0, v=0, T=T_h \tag{5}$$

Where μ is dynamic viscosity, ρ is density, ν is kinematic viscosity, σ is electrical conductivity, k is thermal conductivity, c_p is specific heat, T_0 and T_h are temperature at $y=0$ and $y=\frac{h}{2}$ respectively. Subscripts *thnf* is used for tri-hybrid nanofluid and *f* for base fluid water.

Let stream function such that $u=\frac{\partial \psi}{\partial y}$, $v=-\frac{\partial \psi}{\partial x}$ for eliminating pressure term from equations *(2)* and *(3),* we get

$$u\frac{\partial w}{\partial x}+v\frac{\partial w}{\partial y}=\nu_{thnf}\left(\frac{\partial^2 w}{\partial x^2}+\frac{\partial^2 w}{\partial y^2}\right)-$$
$$-\frac{\partial}{\partial y}\left(\frac{\sigma_{thnf}}{\rho_{thnf}}B_0^2u+\frac{\sigma_{thnf}}{\rho_{thnf}}E_0B_0\mp g\beta_{thnf}(T-T_h)\right) \tag{6}$$

Where w is vorticity, defined as $\mathrm{w}=\frac{\partial \mathrm{v}}{\partial \mathrm{x}}-\frac{\partial \mathrm{u}}{\partial \mathrm{y}}$

Thermophysical properties of nano-particles are given as:

Physical properties	Unit	Base fluid	nanoparticles		
		H_2O	Al_2O_3	Cu	Ni
Dynamic viscosity *(μ)*	$mPas^{-1}$	0.891	-	-	-
Electrical conductivity *(σ)*	$\Omega^{-1}m^{-1}$	0.05	1×10^{-10}	5.96×10^{7}	1.7×10^{7}
Density (ρ)	kgm^{-3}	997.10	3970	8933	8900
Heat Capacity (c_p)	$Jkg^{-1} K^{-1}$	4179	765	385	444
Thermal Conductivity *(k)*	$Wm^{-1} K^{-1}$	0.613	40	401	90.7
Thermal expansion coefficient *(β_T)*	K^{-1}	21×10^{5}	0.85×10^{5}	1.67×10^{5}	134×10^{7}

Thermophysical characteristics of tri-hybrid and hybrid nanofluid are defined as:

Properties	Mono-nanofluid	Hybrid nanofluid	Tri-hybrid nanofluid
Dynamic Viscosity *(μ)*	$\mu_{nf}=\frac{\mu_f}{(1-\phi_1)^{2.5}}$	$\mu_{hnf}=\frac{\mu_f}{(1-\phi_1)^{2.5}(1-\phi_2)^{2.5}}$	$\mu_{thnf}\frac{\mu_f}{(1-\phi_1)^{2.5}(1-\phi_2)^{2.5}(1-\phi_3)^{2.5}}$
Density *(ρ)*	$\rho_{nf}=(1-\phi_1)\rho_f+\phi_1\rho_{n1}$	$\rho_{hnf}=(1-\phi_2)[(1-\phi_1)\rho_f+\phi_1\rho_{n1}]+\phi_2\rho_{n2}$	$\rho_{thnf}=(1-\phi_3)\left((1-\phi_2)[(1-\phi_1)\rho_f+\phi_1\rho_{n1}]+\phi_2\rho_{n2}\right)+\phi_3\rho_{n3}$

Thermal Conductivity *(k)*	$\frac{k_{nf}}{} = \frac{k_{n1}+2k_f-2\phi_1(k_f-k_n}{k_{n1}+2k_f+\phi_1(k_f-k_{n1}}$	$\frac{k_{hnf}}{} = \frac{k_{n2}+2k_{nf}-2\phi_2(k_{nf}-k_{n2})}{k_{n2}+2k_{nf}+\phi_2(k_{nf}-k_{n2})}k_n$	$\frac{k_{thnf}}{} = \frac{k_{n3}+2k_{hnf}-2\phi_2(k_{hnf}-k_{n3})}{k_{n3}+2k_{hnf}+\phi_2(k_{hnf}-k_{n3})}k_{hn}$
Heat capacity *(c_p)*	$(\rho c_p)_{nf} = (1-\phi_1)(\rho c_p)_f + \phi_1(\rho c_p)_{n1}$	$(\rho c_p)_{hnf} = (1-\phi_2)\left[(1-\phi_1)(\rho c_p)_f + \phi_1(\rho c_p)_{n1}\right] + \phi_2(\rho c_p)_{n2}$	$(\rho c_p)_{thnf} = (1-\phi_3)\left((1-\phi_2)\left[(1-\phi_1)(\rho c_p)_f + \phi_1(\rho c_p)_{n1}\right] + \phi_2(\rho c_p)_{n2}\right) + \phi_3(\rho c_p)_{n3}$
Electrical Conductivity *(σ)*	$\frac{\sigma_{nf}}{} = \frac{(1+2\phi_1)\sigma_1+(1-2\phi_1)}{(1-\phi_1)\sigma_1+(1+\phi_1)\sigma_f}$	$\frac{\sigma_{hnf}}{} = \frac{(1+2\phi_2)\sigma_2+(1-2\phi_2)\sigma_{nf}}{(1-\phi_2)\sigma_2+(1+\phi_2)\sigma_{nf}}\sigma_{nf}$	$\frac{\sigma_{thnf}}{} = \frac{(1+2\phi_3)\sigma_3+(1-2\phi_3)\sigma_{hnf}}{(1-\phi_3)\sigma_3+(1+\phi_3)\sigma_{hnf}}\sigma_{hnf}$
Thermal expansion coefficient *(β)*	$(\rho\beta)_{nf} = (1-\phi_1)(\rho\beta)_f + \phi_1(\rho\beta)_{n1}$	$(\rho\beta)_{hnf} = (1-\phi_2)[(1-\phi_1)(\rho\beta)_f + \phi_1(\rho\beta)_{n1}] + \phi_2(\rho\beta)_{n2}$	$(\rho\beta)_{thnf} = (1-\phi_3)([(1-\phi_1)(\rho\beta)_f + \phi_1(\rho\beta)_{n1}] + \phi_2(\rho\beta)_{n2}) + \phi_3(\rho\beta)_{n3}$

Now, the similarity variables are introduced as follow :

$$u = \alpha x f'(\eta), v = -\alpha h f(\eta),$$
$$\theta(\eta) = \frac{T-T_h}{T_0-T_h}, \eta = \frac{y}{h} \quad (7)$$

Using equation (7), equations (4)-(6) are written as:

$$f^{iv} + Re\frac{\nu_f}{\nu_{thnf}}\left(f'f''-ff'''\right) - \frac{\sigma_{thnf}}{\sigma_f}\frac{\mu_f}{\mu_{thnf}}Mf'' + \frac{\sigma_{thnf}}{\sigma_f}\frac{\mu_f}{\mu_{thnf}}EM + \frac{\nu_f}{\nu_{thnf}}\frac{\beta_{thnf}}{\beta_f}\lambda\theta' = 0 \quad (8)$$

$$\frac{k_{thnf}}{k_f}\theta'' - \frac{(\rho c_p)_{thnf}}{(\rho c_p)_f}Prf\theta' + Q\theta + \frac{\sigma_{thnf}}{\sigma_f}MPrEc(f'+E)^2 = 0 \quad (9)$$

With boundary conditions

$$f''(0) = 0, f(0) = 0,$$

$$\theta(0) = 1, f'(1) = 0, f(1) = \frac{1}{2}, \theta(1) = 0 \quad (10)$$

$$Re = \frac{Vh}{\nu_f}, M = \frac{\sigma_f h^2 B_0^2}{\mu_f}, E = \frac{hE_0}{B_0 V x},$$

$$Pr = \frac{\rho c_p h V}{k_f}, Q = \frac{Q_0 h^2}{k_f}, Ec = \frac{V^2 x^2}{h^2 (c_p)_f (T_0 - T_h)},$$

$$\lambda = \frac{Gr}{Re^2}, Gr = \frac{Vh^4 g\beta(T_0-T_h)}{x\nu^3}.$$

Where, V is uniform velocity ($V>0$ suction and $V<0$ injection), Re is Reynolds number, M is magnetic field parameter, E is electric field parameter, Pr is Prandtl number, Ec is Eckert number, λ is thermal buoyancy parameter, Gr is Grashof number.

The skin-friction coefficient C_f and Nusselt number Nu that characterize this study are given by:

$$C_f = \frac{2\mu_{thnf}}{\rho_{thnf}u_0^2}\frac{\partial u}{\partial y}\bigg|_{y=0}$$

$$Nu = \frac{-h}{k_f(T_0-T_h)}(k_{thnf})\frac{\partial T}{\partial y}\bigg|_{y=0} \quad (11)$$

Using *(7)* equation *(11)* can be written as

$$Re_x^{\frac{1}{2}}C_f = -2\frac{\mu_{thnf}}{\mu_f}\frac{\rho_f}{\rho_{thnf}}f''(0)$$

$$Re_x^{-\frac{1}{2}}Nu = -\frac{k_{thnf}}{k_f}\theta'(0). \quad (12)$$

3. Method of solution

Bvp4c program solver in MATLAB software is used to solve the formulated problem. In the first step, the non-linear ordinary differential equation *(9)-(11)* are altered to first order differential equation.

$$\text{Let } f = f1,\ f' = f2,$$

$$f'' = f3, f''' = f4, \theta = f5, \theta' = f6$$

For these assumptions equation *(8)-(10)* will take the following form:

$$f'(1) = f(2)$$

$$f'(2) = f(3)$$

$$f'(3) = f(4)$$

$$f'(4) = -Re\frac{\nu_f}{\nu_{thnf}}(f2f3 - f1f4) + \\ +\frac{\sigma_{thnf}}{\sigma_f}\frac{\mu_f}{\mu_{thnf}}Mf3 - \frac{\sigma_{thnf}}{\sigma_f}\frac{\mu_f}{\mu_{thnf}}EM - \\ -\frac{\nu_f}{\nu_{thnf}}\frac{\beta_{thnf}}{\beta_f}\lambda f$$

$$f'(5) = f(6)$$

$$f'(6) = \\ = \frac{k_f}{k_{thnf}}\left(\frac{(\rho c_p)_{thnf}}{(\rho c_p)_f}Prf1f6 - Qf5 \right. \\ \left. -\frac{\sigma_{thnf}}{\sigma_f}MPrEc(f' + E)^2\right)$$

The boundary conditions (11) are reduced as $f3(0) = 0, f1(0) = 1, f5(0) = 1, f2(1) = 0, f(1) = \frac{1}{2}\ and\ f5(1) = 0$ Now we guess the initial value for the first iteration with mesh size 0.01 and then the first-order equations with boundary conditions are solved by using bvp4c solver in MATLAB software.

4. Results and discussions

To analyse the physical aspects of the considered problem, a comprehensive study have been done. The graphs for fluid velocity and temperature for the different values of physical parameters such as magnetic field parameter *(M),* electric field parameter *(E),* Prandtl number *(Pr),* Eckert number *(Ec),* thermal buoyancy parameter *(λ)* and Grashof number *(Gr)* are shown in Figure *(2-15),* by setting parameter $M=1$, $E=0.1$, $\lambda=0.1$, $Ec=1$, $Pr=1$, $Re=20$, $Q=0.5$. The numerical results for local skin friction and Nusselt number are presented in graphically form. Figure *(2)* demonstrates that enhancing the value of magnetic field parameter *(M)* depreciates the velocity profile near the centreline of the channel and enhances the velocity profile near the channel walls. Since magnetic field is applied normal to the channel walls. Larger values of M increase Lorentz force which enhances the viscosity of the fluid and hence reduces the velocity field. So by controlling the strength of magnetic field, fluid flow in many systems such as MHD power generation, casting of metals etc. can be controlled. The effect of magnetic Field on temperature profile is illustrates via Figure *(3).* Since Lorentz force retards the body force that transverses the motion of the nano particles and this generates more energy dissipation in the fluid model. Hence, by this phenomenon the temperature field increases with growing the values of magnetic field parameter.

Figure *(4, 5)* displays the effect of electric parameter E on velocity and temperature profile. Strong electric field conveys a decline in resistive forces and due to this, motion of nanoparticles in the fluid increases. Hence the velocity profile increases for higher electric field. Strong electric field increases thermal diffusivity of the fluid. Thermal diffusivity is the ratio of thermal conductivity to density and specific heat capacity at a constant pressure. High thermal diffusivity enhances the heat transfer rate and this causes the thermal boundary layer to rise. Hence the temperature profile is also increases for electric field parameter.

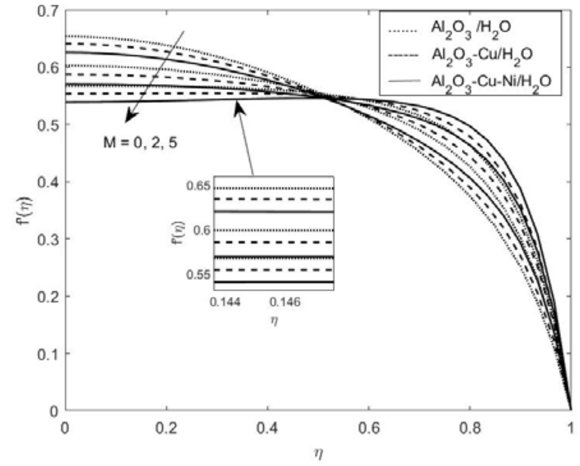

Figure 2 – Effect of M on velocity profile

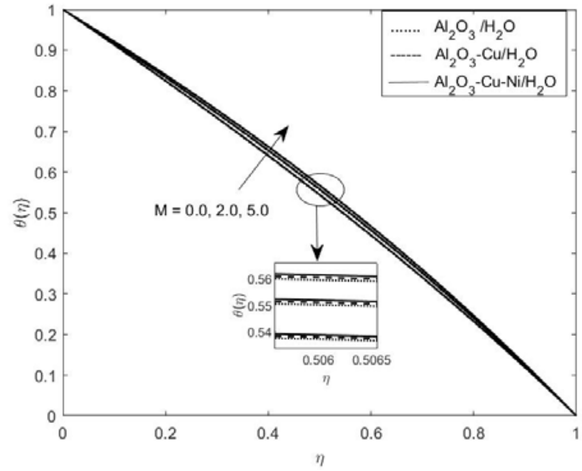

Figure 3 – Effect of M on temperature profile.

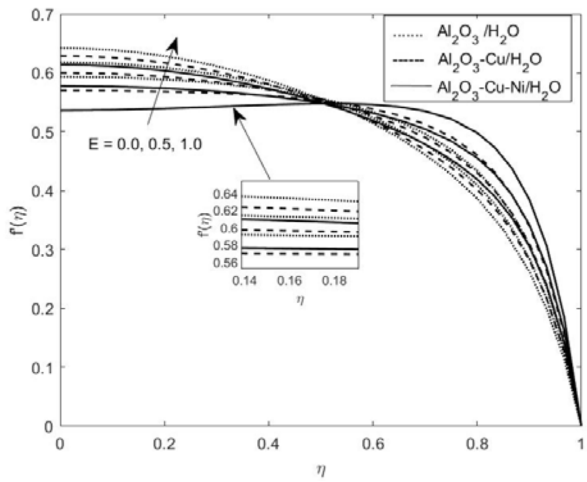

Figure 4 – Effect of E on velocity profile.

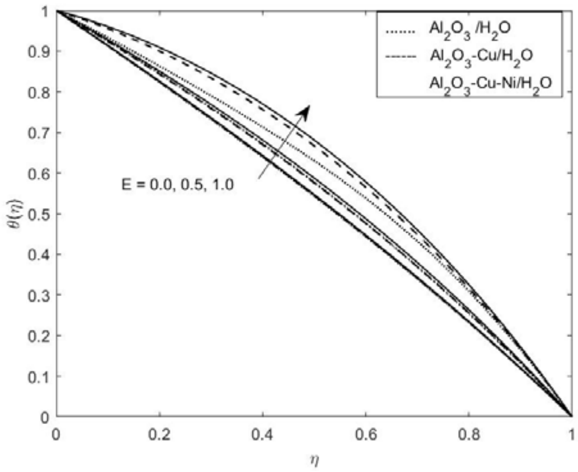

Figure 5 –Effect of E on temperature profile.

It is observed in Figure *(6)* that rising value of Reynolds number *(Re)* reduces the velocity profile near the centreline of the channel and enhances the velocity profile near the channel walls. Since higher Reynolds number drops the viscous forces and generates the stronger inertial forces which increases the fluid density, thus decreases velocity profile. Effect of Prandtl number *(Pr)* on temperature profile is presented in Figure *(7)*. Enhancing the value of Prandtl number *(Pr)* the thermal diffusivity of fluid decreases. Thermal diffusivity is the ratio of thermal conductivity to density and specific heat capacity at a constant pressure. Low thermal diffusivity reduces the heat transfer rate and this causes the thermal boundary layer to drop. Since with higher heat source parameter more energy creates inside the fluid due to heat generation. It causes the growth of thermal boundary layer and hence the temperature field increases with enhancing values of heat source parameter *(Q)* as shown in Figure *(8)*. Figure *(9)*. depicts the effects of Eckert number Ec on the temperature profile $\theta(\eta)$. Since Eckert number (viscous dissipation parameter) is the ratio of advective heat transfer to heat dissipation potential i.e. the transformation of kinetic energy into internal energy. Due to this dissipative heat more heat transfer occurs and thus the thickness of thermal boundary layer increases and the temperature profile increases with increasing Eckert number *Ec*.

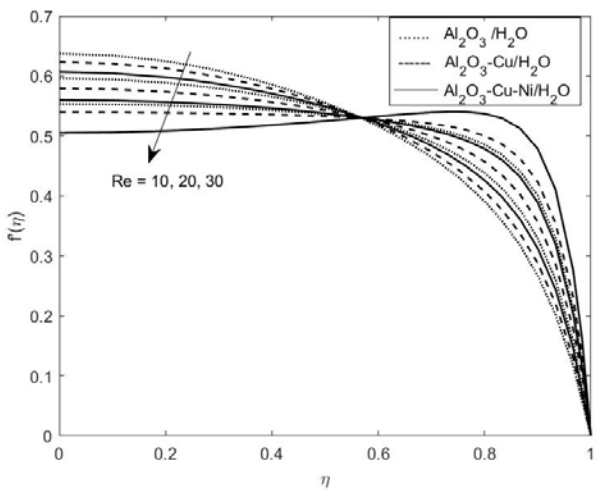

Figure 6 – Effect of Re on velocity profile.

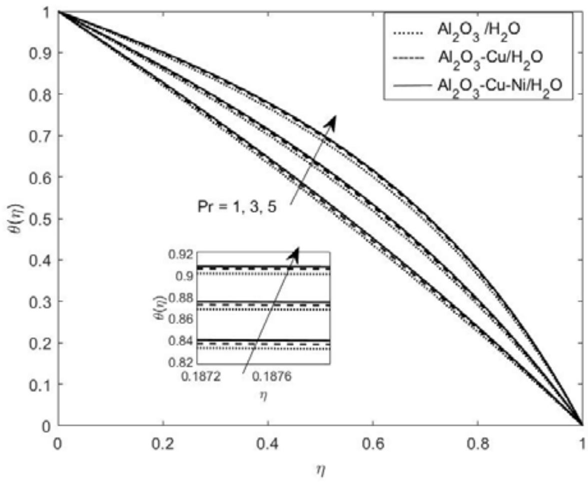

Figure 7 – Effect of Pr on temperature profile.

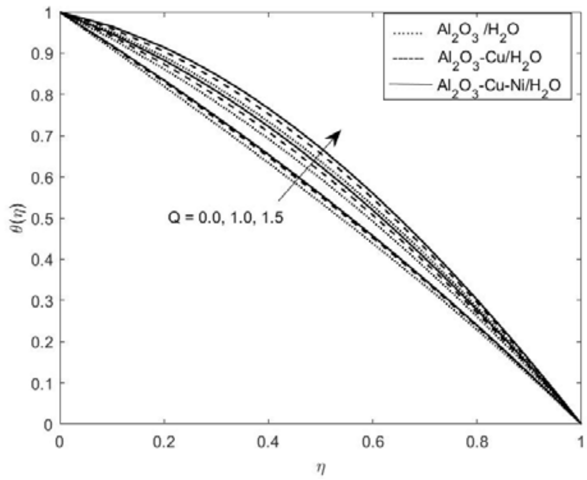

Figure 8 – Effect of Q on temperature profile.

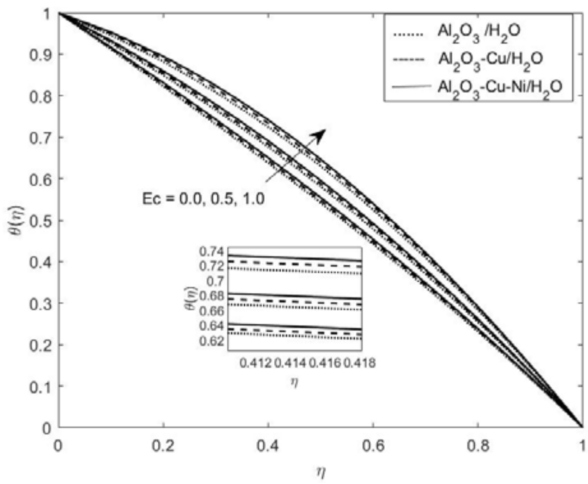

Figure 9 – Effect of Ec on temperature profile.

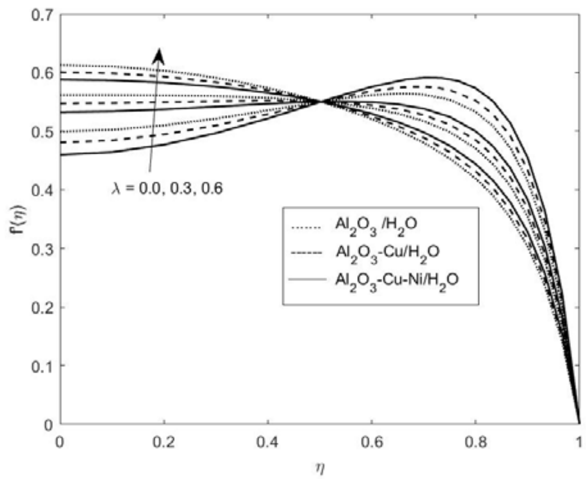

Figure 10 – Effect of λ on velocity profile.

The effect of convection parameter λ on velocity profiles is demonstrated in figure *(10)*. As convection grow, the buoyancy force dominates the viscous force that translates the flow from laminar to turbulent which hastens the flow of the fluid. Figure 10 display the convection has the effect of enhancing the velocity profile.

Comparison for variation in skin-friction coefficient for mono *(Al_2O_3)*, hybrid *(Al_2O_3-Cu)* and ternary nanofluid *(Al_2O_3-Cu-Ni)*, is plotted in figure *(11-15)*. Impact of Reynolds number, electric and magnetic field on skin-friction coefficient is depreciated in figure *(11-12)*. It is observed that the coefficient of skin-friction depreciates with both Reynolds number and magnetic field. While it is found in figure *(12)* that the skin-friction enhances for electric field. The variation in local Nusselt number for various parameters have been depicted in figures *(13-15)*. It is observed that the rate of heat transfer increases electric field, Eckert number and Prandtl number, while decreases for magnetic parameter. Strong electric field increases thermal diffusivity of the fluid. High thermal diffusivity enhances the heat transfer rate and this causes the thermal boundary layer to rise. Eckert number transforms the kinetic energy into internal energy. Due to this dissipative heat more heat transfer occurs.

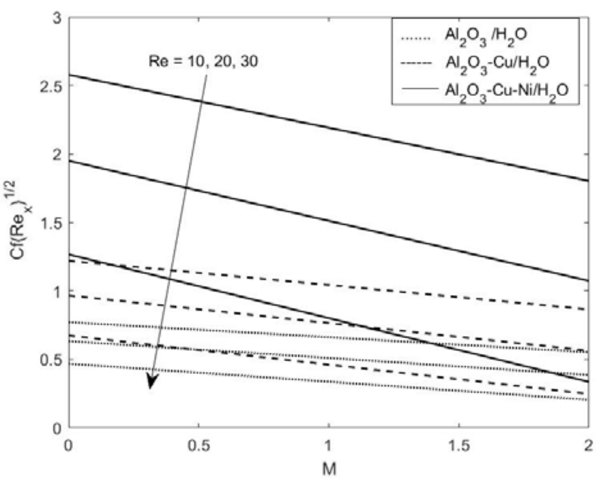

Figure 11 – Effect of Re on skin friction coefficient.

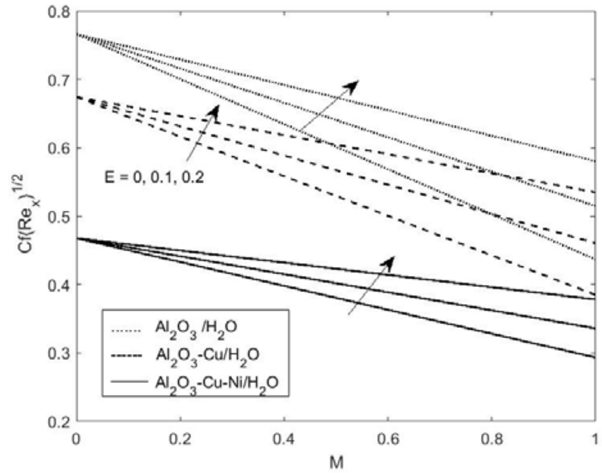

Figure 12 – Effect of E on skin friction coefficient.

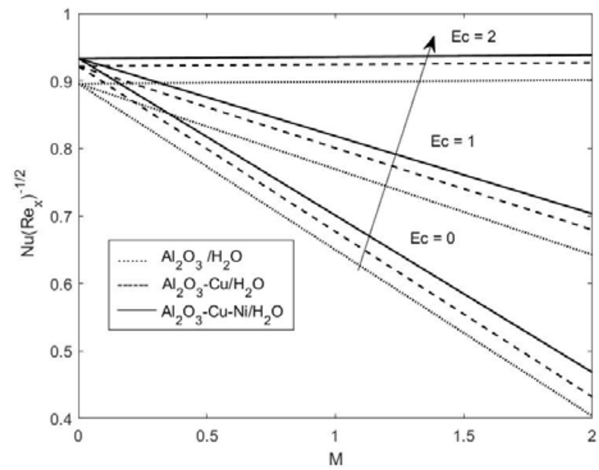

Figure 13 – Effect of Ec on Nusselt number.

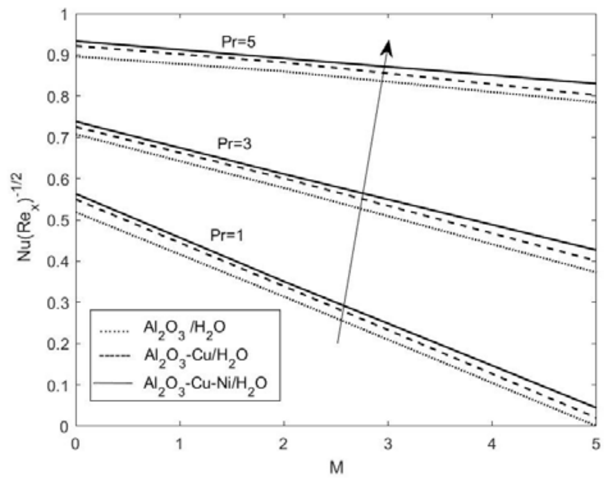

Figure 14 – Effect of Pr on Nusselt number.

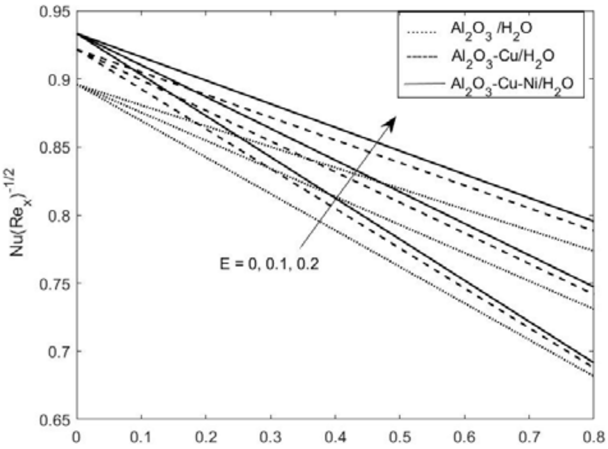

Figure 15 – Effect of E on Nusselt number.

5. Conclusions

A speculative study is done to examine the tri-hybrid nanofluid flow in a convectively heated permeable channel with the effect of heat generation/absorption. The transverse magnetic and electric fields are also considered in the fluid model. A comparative study is carried out for the heat transfer enhancement of base fluid with mono (Al_2O_3), hybrid (Al_2O_3+Cu) and ternary ($Al_2O_3+Cu+Ni$) nanofluids. Notable effect of involved parameters such as magnetic field parameter (M), electric field parameter (E), Prandtl number (Pr), Eckert number (Ec) and thermal buoyancy parameter (λ) on velocity and temperature profiles are analysed and presented in graphical form. The following results are made:

- The effects of involved parameter on tri-hybrid nanofluid are more significant then the mono and hybrid nanofluid.
- The magnetic parameter depreciates the velocity profile and improves temperature profile. While the electric parameter improve the velocity and temperature profiles both.
- Velocity profile enhances with convection parameter and reduces with Reynolds number.
- Temperature profile increases for Prandtl number, Eckert number and for heat source parameter.
- Skin friction coefficient improves for electric parameter and depreciate for magnetic parameter and Reynolds number.
- Nusselt number improves for Eckert number, electric parameter and for Prandtl number, while depreciate for Magnetic parameter.

Conflict of interest

The authors declare no conflict of interest.

References

1. H. K. Gupta, G. Das Agrawal, and J. Mathur, "Investigations for effect of Al2O3-H2O nanofluid flow rate on the efficiency of direct absorption solar collector," *Case Stud. Therm. Eng.*, vol. 5, pp. 70–78, 2015, doi: 10.1016/j.csite.2015.01.002.

2. R. Ali, A. Shahzad, K. us Saher, Z. Elahi, and T. Abbas, "The thin film flow of Al2O3 nanofluid particle over an unsteady stretching surface," *Case Stud. Therm. Eng.*, vol. 29, no. December 2021, pp. 1–13, 2022, doi: 10.1016/j.csite.2021.101695.

3. I. Elbadawy and M. Fayed, "Reliability of Al2O3 nanofluid concentration on the heat transfer augmentation and resizing for single and double stack microchannels," *Alexandria Eng. J.*, vol. 59, no. 3, pp. 1771–1785, 2020, doi: 10.1016/j.aej.2020.04.046.

4. A. Das S. Saha, "Hydrothermal analysis of water-Al2O3 nanofluid flow through a sudden expansion channel with an intermediate step Sandip," vol. 49, no. 4, 2022.

5. U. Rashid and A. Ibrahim, "Impacts of Nanoparticle Shape on Al₂O₃-Water Nanofluid Flow and Heat Transfer over a Non-Linear Radically Stretching Sheet," *Adv. Nanoparticles*, vol. 09, no. 01, pp. 23–39, 2020, doi: 10.4236/anp.2020.91002.

6. K. S. Hwang, S. P. Jang, and S. U. S. Choi, "Flow and convective heat transfer characteristics of water-based Al2O3 nanofluids in fully developed laminar flow regime," *Int. J. Heat Mass Transf.*, vol. 52, no. 1–2, pp. 193–199, 2009, doi: 10.1016/j.ijheatmasstransfer.2008.06.032.

7. M. Mollamahdi, M. Abbaszadeh, and G. A. Sheikhzadeh, "Journal of Heat and Mass Transfer Research Flow Field and Heat Transfer in a Channel with a Permeable Wall Filled with Al 2 O 3 -Cu / Water Micropolar Hybrid Nanofluid , Effects of Chemical Reaction and Magnetic Field," vol. 3, pp. 101–114, 2016, doi: 10.22075/jhmtr.2016.447.

8. M. Khoshvaght-Aliabadi, "Influence of different design parameters and Al2O3-water nanofluid flow on heat transfer and flow characteristics of sinusoidal-corrugated channels," *Energy Convers. Manag.*, vol. 88, pp. 96–105, 2014, doi: 10.1016/j.enconman.2014.08.042.

9. A. Prakash, S. Satsangi, S. Mittal, B. Nigam, P. K. Mahto, and B. P. Swain, "Investigation on Al2O3 Nanoparticles for Nanofluid Applications- A Review," *IOP Conf. Ser. Mater. Sci. Eng.*, vol. 377, no. 1, 2018, doi: 10.1088/1757-899X/377/1/012175.

10. A. Magesh, P. Tamizharasi, and R. Vijayaragavan, "MHD flow of (Al2O3/H2O) nanofluid under the peristaltic mechanism in an asymmetric channel," *Heat Transf.*, vol. 51, no. 7, pp. 6563–6577, 2022, doi: https://doi.org/10.1002/htj.22613.

11. K. V. Sharma, L. S. Sundar, and P. K. Sarma, "Estimation of heat transfer coefficient and friction factor in the transition flow with low volume concentration of Al2O3 nanofluid flowing in a circular tube and with twisted tape insert," *Int. Commun. Heat Mass Transf.*, vol. 36, no. 5, pp. 503–507, 2009, doi: 10.1016/j.icheatmasstransfer.2009.02.011.

12. M. Sheikholeslami, M. B. Gerdroodbary, R. Moradi, A. Shafee, and Z. Li, "Application of Neural Network for estimation of heat transfer treatment of Al[Formula presented]O[Formula presented]-H[Formula presented]O nanofluid through a channel," *Comput. Methods Appl. Mech. Eng.*, vol. 344, pp. 1–12, 2019, doi: 10.1016/j.cma.2018.09.025.

13. N. A. L. Aladdin, N. Bachok, and I. Pop, "Cu-Al2O3/water hybrid nanofluid flow over a permeable moving surface in presence of hydromagnetic and suction effects," *Alexandria Eng. J.*, vol. 59, no. 2, pp. 657–666, 2020, doi: 10.1016/j.aej.2020.01.028.

14. N. Safwa, I. Waini, N. Arifin, and I. Pop, "Unsteady squeezing flow of Cu - Al 2 O 3 / water hybrid nanofluid in a horizontal channel with magnetic field," *Sci. Rep.*, pp. 1–11, 2021, doi: 10.1038/s41598-021-93644-4.

15. F. Saba, N. Ahmed, U. Khan, A. Waheed, M. Rafiq, and S. T. Mohyud-Din, "Thermophysical analysis of water based (Cu-Al2O3) hybrid nanofluid in an asymmetric channel with dilating/squeezing walls considering different shapes of nanoparticles," *Appl. Sci.*, vol. 8, no. 9, 2018, doi: 10.3390/app8091549.

16. S. Das, R. N. Jana, and O. D. Makinde, "MHD Flow of Cu-Al2O3/Water hybrid nanofluid in porous channel: Analysis of entropy generation," *Defect Diffus. Forum*, vol. 377, pp. 42–61, 2017, doi: 10.4028/www.scientific.net/DDF.377.42.

17. U. Khan *et al.*, "A novel hybrid model for Cu-Al2O3/H2O nanofluid flow and heat transfer in convergent/divergent channels," *Energies*, vol. 13, no. 7, 2020, doi: 10.3390/en13071686.

18. Adnan *et al.*, "Thermal efficiency in hybrid (Al2O3-CuO/H2O) and tri-hybrid (Al2O3-CuO-Cu/H2O) nanofluids between converging/diverging channel with viscous dissipation function: Numerical analysis," *Front. Chem.*, vol. 10, no. August, pp. 1–12, 2022, doi: 10.3389/fchem.2022.960369.

19. M. B. Wollele, H. H.V, and M. Assaye, "Heat transfer augmentation of Al2O3-Cu/water hybrid nanofluid in circular duct with inserts," *Cogent Eng.*, vol. 9, no. 1, 2022, doi: 10.1080/23311916.2022.2146627.

20. M. Ghalambaz, S. Mohsen, H. Zadeh, A. Veismoradi, M. A. Sheremet, and I. Pop, "Odd-Shaped Cavity Filled with a Cu-Al 2 O 3 Hybrid Nanofluid," 2021, [Online]. Available: https://doi.org/10.3390/sym13010122

21. Z. Xuan, Y. Zhai, M. Ma, Y. Li, and H. Wang, "Thermo-economic performance and sensitivity analysis of ternary hybrid nanofluids," *J. Mol. Liq.*, vol. 323, p. 114889, 2021, doi: 10.1016/j.molliq.2020.114889.

22. A. Thakur and S. Sood, "Tri-Hybrid Nanofluid Flow Towards Convectively Heated Stretching Riga Plate with Variable Thickness," *J. Nanofluids*, vol. 12, no. 4, pp. 1129–1140, 2023, doi: 10.1166/jon.2023.1990.

23. K. Guedri *et al.*, "Thermally Dissipative Flow and Entropy Analysis for Electromagnetic Trihybrid Nanofluid Flow Past a Stretching Surface," *ACS Omega*, vol. 7, no. 37, pp. 33432–33442, 2022, doi: 10.1021/acsomega.2c04047.

24. Z. Mahmood, S. M. Eldin, K. Rafique, and U. Khan, "Numerical analysis of MHD tri-hybrid nanofluid over a nonlinear stretching/shrinking sheet with heat generation/absorption and slip conditions," *Alexandria Eng. J.*, vol. 76, pp. 799–819, 2023, doi: 10.1016/j.aej.2023.06.081.

25. K. Guedri, A. Khan, N. Sene, Z. Raizah, A. Saeed, and A. M. Galal, "Thermal Flow for Radiative Ternary Hybrid Nanofluid over Nonlinear Stretching Sheet Subject to Darcy-Forchheimer Phenomenon," *Math. Probl. Eng.*, vol. 2022, 2022, doi: 10.1155/2022/3429439.

26. S. Das, A. Ali, R. N. Jana, and O. D. Makinde, "EDL impact on mixed magneto-convection in a vertical channel using ternary hybrid nanofluid," *Chem. Eng. J. Adv.*, vol. 12, no. September, p. 100412, 2022, doi: 10.1016/j.ceja.2022.100412.

27. S. Bilal, M. I. Asjad, S. ul Haq, M. Y. Almusawa, E. S. M. Tag-ElDin, and F. Ali, "Significance of Dufour and Soret aspects on dynamics of water based ternary hybrid nanofluid flow in a 3D computational domain," *Sci. Rep.*, vol. 13, no. 1, pp. 1–20, 2023, doi: 10.1038/s41598-023-30609-9.

28. G. K. Ramesh, J. K. Madhukesh, S. A. Shehzad, and A. Rauf, "Ternary nanofluid with heat source/sink and porous medium effects in stretchable convergent/divergent channel," *Proc. Inst. Mech. Eng. Part E J. Process Mech. Eng.*, vol. 0, no. 0, p. 09544089221081344, doi: 10.1177/09544089221081344.

29. A. Rauf, Faisal, N. A. Shah, and T. Botmart, "Hall current and morphological effects on MHD micropolar non-Newtonian tri-hybrid nanofluid flow between two parallel surfaces," *Sci. Rep.*, vol. 12, no. 1, pp. 1–20, 2022, doi: 10.1038/s41598-022-19625-3.

30. S. Manjunatha, V. Puneeth, B. J. Gireesha, and A. J. Chamkha, "Theoretical Study of Convective Heat Transfer in Ternary Nanofluid Flowing past a Stretching Sheet," *J. Appl. Comput. Mech.*, vol. 8, no. 4, pp. 1279–1286, 2022, doi: 10.22055/JACM.2021.37698.3067.

31. M. Z. U. Abideen, M. Faisal, and M. Z. Akbar, "Magnetized Tri-hybrid Nanofluids flow with binary Chemical Reaction and activation Energy through the porous Surfaces," *Math. Sci. Appl.*, vol. 1, no. 1, pp. 1–17, 2022, doi: 10.52700/msa.v1i1.1.

32. M. F. Najafabadi, H. TalebiRostami, K. Hosseinzadeh, and D. D. Ganji, "Investigation of nanofluid flow in a vertical channel considering polynomial boundary conditions by Akbari-Ganji's method," *Theor. Appl. Mech. Lett.*, vol. 12, no. 4, p. 100356, 2022, doi: 10.1016/j.taml.2022.100356.

33. H. Maiti and S. Mukhopadhyay, "Existence of MHD boundary layer hybrid nanofluid flow through a divergent channel with mass suction and injection," *Chem. Eng. J. Adv.*, vol. 14, p. 100475, 2023, doi: https://doi.org/10.1016/j.ceja.2023.100475.

34. J. Raza, A. M. Rohni, and Z. Omar, "Multiple Solutions of Mixed Convective MHD Casson Fluid Flow in a Channel," *J. Appl. Math.*, vol. 2016, 2016, doi: 10.1155/2016/7535793.

35. M. Kumari and S. Jain, "Radiative flow of MHD casson fluid between two permeable channels filled with porous medium and non-linear chemical reaction," *Int. J. Adv. Sci. Technol.*, vol. 29, no. 8 Special Issue, pp. 838–845, 2020.

36. I. Siddique, K. Sadiq, F. Jarad, M. K. Al Mesfer, M. Danish, and S. Yaqoob, "Analysis of Natural Convection in Nanofluid Flow through a Channel with Source/Sink Effect," *J. Nanomater.*, vol. 2022, 2022, doi: 10.1155/2022/2738398.

37. Y. Zheng, H. Yang, H. Mazaheri, A. Aghaei, N. Mokhtari, and M. Afrand, "An investigation on the influence of the shape of the vortex generator on fluid flow and turbulent heat transfer of hybrid nanofluid in a channel," *J. Therm. Anal. Calorim.*, vol. 143, no. 2, pp. 1425–1438, 2021, doi: 10.1007/s10973-020-09415-2.

38. Zeeshan, N. A. Ahammad, N. A. Shah, J. D. Chung, Attaullah, and H. U. Rasheed, "Analysis of Error and Stability of Nanofluid over Horizontal Channel with Heat/Mass Transfer and Nonlinear Thermal Conductivity," *Mathematics*, vol. 11, no. 3, 2023, doi: 10.3390/math11030690.

39. M. A. Ahmed, N. H. Shuaib, M. Z. Yusoff, and A. H. Al-Falahi, "Numerical investigations of flow and heat transfer enhancement in a corrugated channel using nanofluid," *Int. Commun. Heat Mass Transf.*, vol. 38, no. 10, pp. 1368–1375, 2011, doi: 10.1016/j.icheatmasstransfer.2011.08.013.

40. L. Verma, R. Meher, Z. Hammouch, and H. M. Baskonus, "Effect of heat transfer on hybrid nanofluid flow in converging/diverging channel using fuzzy volume fraction," *Sci. Rep.*, vol. 12, no. 1, pp. 1–21, 2022, doi: 10.1038/s41598-022-24259-6.

41. I. Tlili, N. N. Hamadneh, W. A. Khan, and S. Atawneh, "Thermodynamic analysis of MHD Couette–Poiseuille flow of water-based nanofluids in a rotating channel with radiation and Hall effects," *J. Therm. Anal. Calorim.*, vol. 132, no. 3, pp. 1899–1912, 2018, doi: 10.1007/s10973-018-7066-5.

42. K. K. Asogwa, B. S. Goud, Y. D. Reddy, and A. A. Ibe, "Suction effect on the dynamics of EMHD casson nanofluid over an induced stagnation point flow of stretchable electromagnetic plate with radiation and chemical reaction," *Results Eng.*, vol. 15, no. July, p. 100518, 2022, doi: 10.1016/j.rineng.2022.100518.

43. A. Wakif, A. Chamkha, I. L. Animasaun, M. Zaydan, H. Waqas, and R. Sehaqui, "Novel Physical Insights into the Thermodynamic Irreversibilities Within Dissipative EMHD Fluid Flows Past over a Moving Horizontal Riga Plate in the Coexistence of Wall Suction and Joule Heating Effects: A Comprehensive Numerical Investigation," *Arab. J. Sci. Eng.*, vol. 45, no. 11, pp. 9423–9438, 2020, doi: 10.1007/s13369-020-04757-3.

44. M. M. Bhatti, A. Zeeshan, and R. Ellahi, "Electromagnetohydrodynamic (EMHD) peristaltic flow of solid particles in a third-grade fluid with heat transfer," *Mech. Ind.*, vol. 18, no. 3, 2017, doi: 10.1051/meca/2016061.

45. K. Tian, S. An, G. Zhao, and Z. Ding, "Two-Dimensional Electromagnetohydrodynamic (EMHD) Flows of Fractional Viscoelastic Fluids with Electrokinetic Effects," *Nanomaterials*, vol. 12, no. 19, pp. 1–16, 2022, doi: 10.3390/nano12193335.

46. M. Rashid, I. Shahzadi, and S. Nadeem, "Significance of Knudsen number and corrugation on EMHD flow under metallic nanoparticles impact," *Phys. A Stat. Mech. its Appl.*, vol. 551, p. 124089, 2020, doi: 10.1016/j.physa.2019.124089.

47. E. A. Algehyne, A. F. Alharbi, A. Saeed, A. Dawar, P. Kumam, and A. M. Galal, "Numerical analysis of the chemically reactive EMHD flow of a nanofluid past a bi-directional Riga plate influenced by velocity slips and convective boundary conditions," *Sci. Rep.*, vol. 12, no. 1, pp. 1–15, 2022, doi: 10.1038/s41598-022-20256-x.

48. S. Khatun, M. M. Islam, M. T. Mollah, S. Poddar, and M. M. Alam, "EMHD radiating fluid flow along a vertical Riga plate with suction in a rotating system," *SN Appl. Sci.*, vol. 3, no. 4, pp. 1–14, 2021, doi: 10.1007/s42452-021-04444-4.